Hindawi
Geofluids
Volume 2022, Article ID 7151294, 8 pages
https://doi.org/10.1155/2022/7151294

Research Article

Analysis of Blasting Vibration Effect of Railway Tunnel and Determination of Reasonable Burial Depth

Hailong Wang,[1,2] Yan Zhao,[1] Renliang Shan,[1] Xiao Tong,[1] and Dong Liu[1]

[1]*School of Mechanics and Civil Engineering, China University of Mining and Technology (Beijing), Beijing 100083, China*
[2]*Department of Civil Engineering, Hebei University of Architecture, HeBei, 075000, China*

Correspondence should be addressed to Yan Zhao; 304965624@qq.com

Received 25 May 2022; Revised 2 August 2022; Accepted 20 August 2022; Published 16 September 2022

Academic Editor: Qibin Lin

Based on specific examples of underpass tunnel blasting, field measurements, and numerical simulation studies are carried out. According to the results of the blasting vibration data measured on-site, a regression model of the blasting vibration velocity is established. Based on the wavelet packet energy spectrum analysis method, the effect of frequency on the vibration response intensity is studied. In addition, the maximum charge per delay allowed for tunnel blasting is obtained by formula inversion. Relying on ANSYS/LS-DYNA to establish a three-dimensional numerical model, the accuracy of numerical simulation can be checked by the measured vibration data. The results show that the numerical simulation has high precision and can meet the subsequent analysis needs. Using numerical simulation, the variation law of the vibration response characteristics of ground blasting under different tunnel burial depths is studied. The analysis results show that with increasing tunnel burial depth, the ground blasting vibration velocity decays exponentially. According to the corresponding specification of blasting vibration, a reasonable value range of the buried depth of the underpass tunnel can be obtained. The research ideas and methods introduced can be used for reference for similar railway tunnel blasting control and railway tunnel route selection.

1. Introduction

China's transportation infrastructure construction is entering an era of rapid development. As an important form of transportation infrastructure, mountain tunnels are widely used in highway and railway projects. The drill-and-blast method has the advantages of good economic benefits, simple operation, and so on. Therefore, it is widely used in the excavation process of mountain tunnels. However, blasting vibration, air pollution, and noise caused by blasting construction will all have adverse effects on the surrounding environment. For example, if the vibration intensity exceeds the control threshold, it will directly affect the structural stability of the existing building and even threaten its safety.

A large number of scholars [1–4] have conducted related studies on the analysis of the blasting vibration effect of mountain tunnels. Qin and Zhang [5] found that there is a good fitting relationship between the peak blasting vibration velocity and the total charge. Zhao et al. [6] systematically studied the attenuation law of the blasting vibration of the initial tunnel support based on signal processing technology and obtained a model equation that can characterize blasting energy changes. Conducted a theoretical analysis of the measured waveform and combined the method of dimensional analysis to obtain the analytical solution of the wave corresponding to cutting and blasting. Tian et al. [7] studied the propagation law of blasting vibration in parallel small-distance tunnels through wavelet packet analysis. The results show that the dominant frequency band of far-field blasting vibration is mainly concentrated in the low-frequency range. The analysis results show that the vibration energy is proportional to the square of the blasting vibration velocity. Wang et al. [8] elaborated the blasting vibration control of a three-dimensional intersection tunnel in detail and achieved a good control effect. In addition, modern technologies [2] represented by machine learning [9] are also widely used in research in this field. Hasanipanah et al. [10] made a prediction and analysis of ground vibration caused by blasting construction based on particle swarm optimization and achieved good results. Based on the intelligent algorithm of

extreme learning machine, Jahed et al. [1] carried out prediction research on mine blasting vibration.

The above studies have analyzed the blasting vibration effect by means of on-site monitoring, numerical simulation, or machine learning. However, there are few reports on the analysis of the blasting vibration effect of the underpass tunnel and the determination of the reasonable burial depth of the tunnel. In the actual highway and railway tunnel projects, on the premise of ensuring the safety of surrounding buildings, it is an indispensable work to scientifically and reasonably divide the blasting vibration affected area. Therefore, according to a railway tunnel project, it is imminent to systematically analyze the blasting vibration caused by tunnel blasting. For the actual blasting project, the choice of tunnel depth should be an important part of this research.

The article mainly elaborates the content through the following three main aspects: first, relying on the specific railway tunnel project, the corresponding blasting vibration in-situ test is carried out to obtain the characteristic information in the time domain and frequency domain of blasting vibration response; secondly, through the LS-DYNA simulation platform, a three-dimensional numerical model is proposed and checked with the test results; and finally, we carry out a numerical simulation study, mainly analyzing the relationship between the tunnel burial depth and the corresponding blasting vibration response in order to provide suggestions for the selection of the burial depth of similar railway tunnels in the future.

2. Project Overview and On-Site Monitoring

2.1. Engineering Conditions. As shown in Figure 1, the Tai-Xi Railway under construction is an important traffic channel connecting Zhangjiakou, Hebei, and Inner Mongolia. In this paper, an example of a mountain tunnel in the Tai-Xi Railway is used as the engineering background to analyze the blasting vibration effect.

The tunnel mainly connects Tai Zi Cheng Station and the newly built Chong Li Station, with a total length of 5490 m. As shown in Figure 2, part of the main tunnel penetrates the existing village. The minimum vertical clear distance between the village ground and the top of the tunnel is approximately 25 m. Geological exploration data show that the surrounding rock of the tunnel in the underpass area is mainly of grade IV.

During the blasting vibration construction period, the development of cracks in existing buildings was investigated. The results of the survey found that the main structural forms are civil structures, stone-wood structures, brick-earth-wood hybrid structures, and brick-wood structures. Moreover, most houses do not have earthquake-resistance measures, and the overall quality is generally poor.

According to the "Blasting Safety Regulations" GB6722-2014, the blasting vibration speed control threshold V_{max} is selected according to the protection object categories of earthen caves, adobe houses, and rubble houses, which is 1.5 cm/s.

The blasting construction uses the full-section method to excavate, and the cycling footage is 2.8~3.6 m. This project adopts a millisecond detonator delay. The specific blasthole arrangement is shown in Figure 3.

Figure 1: Panoramic route map of the Tai-Xi Railway.

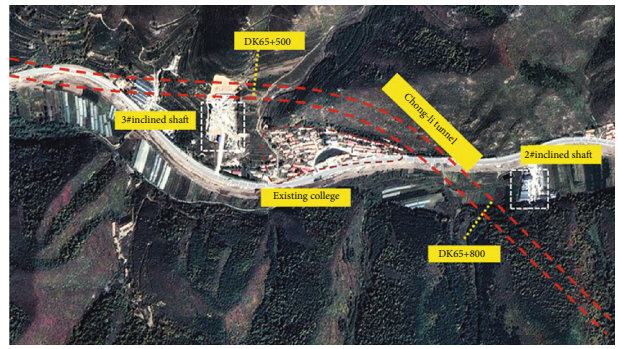

Figure 2: Plan location map of the underpass railway tunnel.

2.2. Monitoring Plan. From October 19, 2020 to December 2, 2020, the researchers conducted a total of 35 field monitoring experiments. During the field monitoring process, researchers selected a certain number of measuring points in the existing villages for research. This vibration monitoring uses the TC-4850 N blasting vibrometer developed by Zhongke Speed Control Company. Also, each vibrometer is equipped with a TCS-B3 speed sensor. During on-site installation, first, surface debris should be removed at the monitoring point. Then, the vibration velocity sensor is rigidly attached to the ground with plaster.

The location and arrangement of the specific measuring points are shown in Figure 4.

3. Analysis of Blasting Vibration Response Characteristics

3.1. Analysis of Blasting Vibration Velocity. From October 19 to December 2 in 2020, a total of 32 blasting vibration field

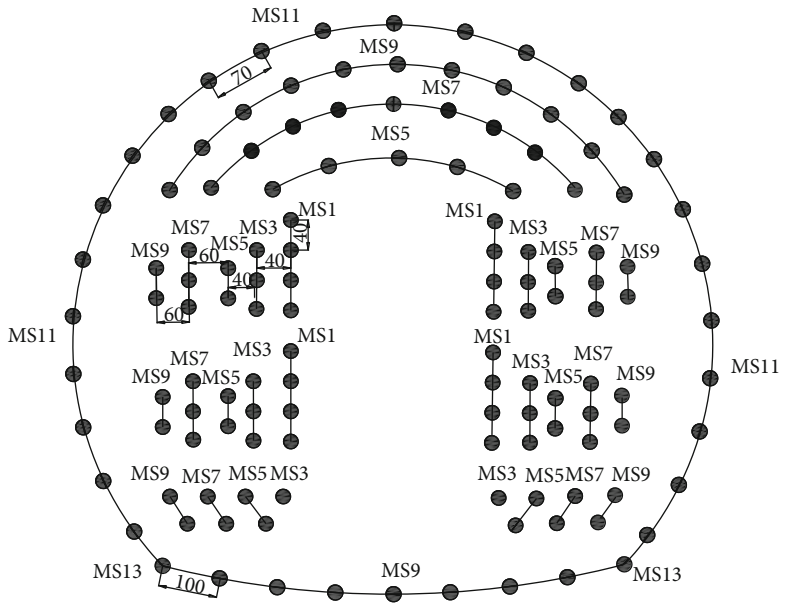

Figure 3: Layout of the blast hole.

Figure 4: Layout of measuring points.

monitoring tests were conducted. Due to space limitations, three representative experimental results were selected for research, as shown in Table 1. Figure 5 shows that all the time-history curves in the three directions have 7 clear peaks, which correspond to the positions of the detonators. Compared with the vibration speeds in the three directions, the vibration speed in the vertical direction is the largest. Following the "Blasting Safety Regulations" GB6722-2014 (2015), only the peak vibration velocity of the particle in the vertical direction will be analyzed in the follow-up.

As shown in Table 1, measurement point #1 has the largest blasting vibration response and is most significantly affected by blasting construction. In the two blasting tests, the blasting peak vibration velocities of measuring point #1 are 1.99 cm/s and 2.33 cm/s, respectively, with both exceeding the specified control standards. It should be pointed out that the peak value of blasting vibration velocity is represented by PPV in the following text.

It should be emphasized that the measured data in this paper came from the blasting vibration monitoring experiment of the Chong-li tunnel.

The magnitude of the blasting vibration peak velocity is affected by many factors, such as the amount of charge, blasting distance, and engineering geological conditions [11, 12]. It is well known that the blasting peak vibration velocity is proportional to the maximum charge per delay and inversely proportional to the distance from the blasting point. Chinese and Russian researchers often use Sadowski's

Table 1: Measured peak blasting vibration velocity.

Field experiment	Measuring point	The distance from explosion/R (m)	PPV (cm/s)
I	#1	27.58	1.99
	#2	30.48	1.66
	#3	36.89	1.34
	#4	40.31	1.11
	#5	49.24	1.00
II	#1	25.49	2.33
	#2	27.54	2.25
	#3	31.26	1.91
	#4	36.28	1.46
	#5	42.48	1.35
III	#1	29.02	1.92
	#2	33.45	1.70
	#3	38.04	1.52
	#4	45.55	1.31
	#5	50.03	1.17
IV	#1	30.55	1.86
	#2	36.22	1.53
	#3	42.16	1.46
	#4	50.32	1.20
	#5	57.84	0.92
V	#1	28.28	1.96
	#2	31.33	1.62
	#3	38.54	1.49
	#4	41.66	1.30
	#5	47.20	1.20

formula [13] to predict the transmission law of blasting vibration.

$$\mathrm{PPV} = K\left(\frac{\sqrt[3]{Q}}{R}\right)^{\alpha}, \tag{1}$$

where Q represents the maximum charge per delay, R represents the distance from the explosion, and K and α represent the site coefficient and attenuation coefficient related to the blasting vibration law, respectively.

Taking the natural logarithm on both sides of Equation (1), we can get

$$\ln(\mathrm{PPV}) = \alpha \ln\left(\frac{Q^{1/3}}{R}\right) + \ln(K). \tag{2}$$

Based on the measured data in Table 1, we obtain the following model equation by linear fitting:

$$y = 0.851x + 2.394. \tag{3}$$

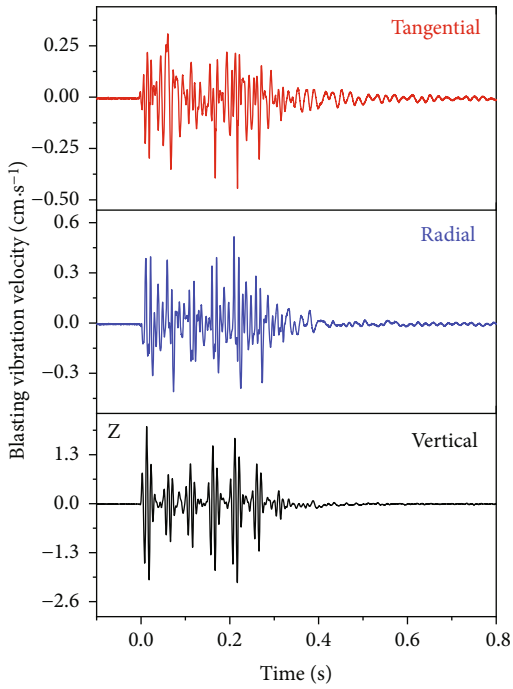

Figure 5: Time-history waveform of the blasting vibration of the experiment.

Equation (3) can also be expressed as

$$\mathrm{PPV} = 10.957\left(\frac{\sqrt[3]{Q}}{R}\right)^{0.851}. \tag{4}$$

Figure 6 shows that the correlation coefficient of Formula (4) is as high as 0.907, indicating that the fitting of Formula (4) is of high accuracy, which can reflect the attenuation law of blasting vibration.

3.2. Analysis of Blasting Vibration Frequency. A large number of studies [14, 15] have shown that the blasting vibration response is not only related to the vibration velocity but also affected by the blasting vibration frequency. In some countries, the influence of vibration frequency is also taken into consideration when issuing new blasting vibration control regulations. At present, research on the blasting vibration frequency is mainly realized by means of signal analysis. Compared with fast Fourier analysis and wavelet transform, wavelet packet analysis [16] can reflect the distribution characteristics of both the frequency domain and time domain of the signal and improve the resolution of the high-frequency signal.

Assuming that an n-level decomposition of the burst signal with frequency ω results in 2^n subbands, with each subband width being $\omega/2^n$ [8]

$$x(t) = \sum_{j}^{2n} x_{n,j}. \tag{5}$$

Let $E_{n,j}$ represent the signal energy value corresponding

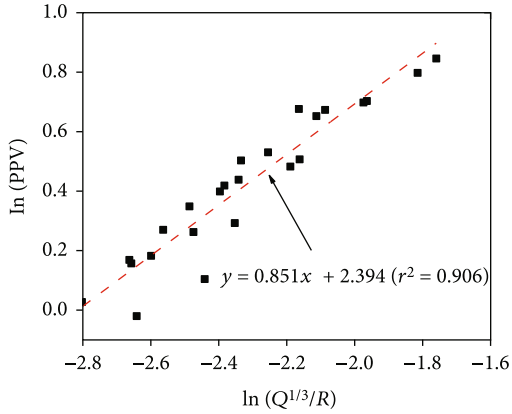

Figure 6: Fitting curve of the blasting vibration velocity.

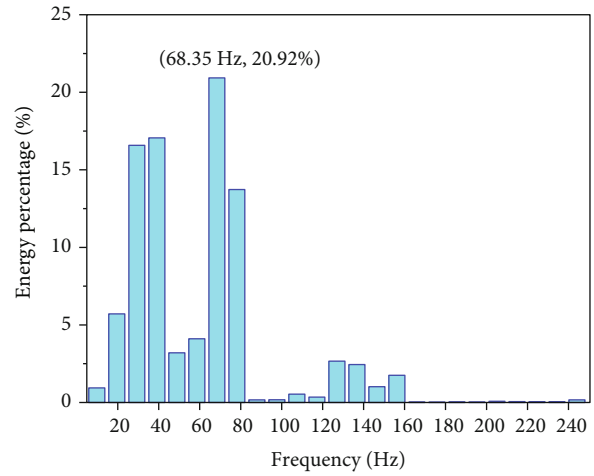

Figure 7: The energy spectrum of blasting vibration.

to the frequency band of $x_{n,j}$ gives [14].

$$E_{n,j} = \int \left|x_{j,i}(t)\right|^2 dt = \sum_{k=1}^{m} \left|z_{i,k}\right|^2, \tag{6}$$

where $z_{i,k}$ is the amplitude corresponding to the discrete points of the subband, k is the number of discrete points, and m is the length of the collected data.

The total vibration energy of the blasting signal can be expressed as [17]

$$E = \sum_{j=1}^{2j} E_{n,j}. \tag{7}$$

The energy percentage of each frequency ($T_{n,j}$) band can be expressed as follows [18, 19]:

$$T_{n,j} = \frac{E_{n,j}}{E}. \tag{8}$$

Based on Formula (5)–(8), the code is written through the MATLAB platform. The measured blasting vibration signal is decomposed by 9 layers of wavelet packets, and the corresponding spectral energy distribution is obtained as shown in Figure 7.

The field experiment results show that the vibration data of multiple measuring points have exceeded the vibration control threshold, so relevant vibration reduction measures must be taken to control the blasting.

Under the condition of maximum peak vibration velocity (1.5 cm/s) and minimum distance from explosion, which is equal to the clear vertical distance (25 m), the maximum allowable charge per delay is 21.49 kg according to Formula (4).

4. Numerical Simulation

4.1. Establishment of Numerical Simulation Model. Due to factors like the number of measuring points, monitoring environment, and human error, data obtained through field measurements is insufficient for the comprehensive investigation. Therefore, the authors establish a three-dimensional numerical model based on ANSYS/LS-DYNA and deeply discuss the influence of blasting vibration on the surrounding existing buildings.

Considering the symmetry, only half of the model is built, as shown in Figure 8, whose length, width, and height are 25 m, 50 m, and 65 m, respectively. The tunnel radius is 6 m. Affected by the rock clamping effect and the amount of charge, the blasting vibration response induced by bench cutting blasting in the tunnel is the largest. Therefore, the numerical analysis only studies the vibration caused by tunnel cutting blasting.

This simulation uses an 8-node solid element solid164, and the unit system consists of cm, g, and μs. The numerical model has a total of 13052501 nodes and 2255592 elements. To eliminate any influence of the reflection and refraction of the stress wave at boundaries on the numerical results, nonreflection boundaries are applied to the side and bottom surfaces. In addition, a symmetric displacement constraint in the X direction is imposed on the symmetry plane. To approach real engineering practice, the top surface of the model is set as a free boundary.

Model materials mainly include tunnel surrounding rock, gun mud, explosives, and air. The Lagrange algorithm is used for the surrounding rock and taphole mud of the tunnel. Explosives and air are defined as fluids by the ALE algorithm. The ALE method is suitable for numerical simulation of fluid dynamics problems. In the ALE algorithm, the grid can be properly adjusted in the calculation process according to the defined parameters to prevent the generation of grid distortion. This method is very beneficial when analyzing large deformation problems because the default mesh-to-mesh flow is free with this method.

The tunnel surrounding rock adopts the isotropic plastic kinematic hardening model ∗MAT_PLASTIC_KINEMATIC to describe the stress–strain relationship of the rock mass under the action of blasting vibration, and the ∗MAT_ADD_EROSION keyword is added to reflect the failure of the rock mass. The mechanical properties of the rock, obtained in laboratory tests, are shown in Table 2.

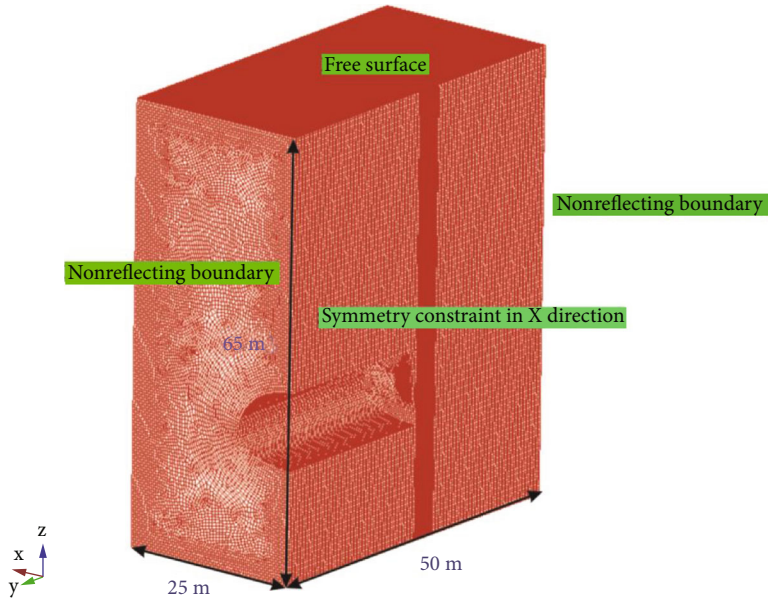

Figure 8: LS-DYNA 3D numerical model.

Table 2: Calculation parameters of the rock surrounding the tunnel.

Density/kg·m^{-3}	Young's modulus/GPa	Poisson's ratio	Yield strength/MPa
2690	45	0.25	85

In ANSYS/LS-DYNA, the whole process of the explosive explosion is simulated by setting the corresponding state equation. The Jones–Wilkens–Lee equation of state is widely used to model the relationship between pressure and specific volume during an explosion. The specific representation form is as follows:

$$P = A\left(1 - \frac{\omega}{R_1 V}\right)e^{-R_1 V} + B\left(1 - \frac{\omega}{R_2 V}\right)e^{-R_2 V} + \frac{\omega E_0}{V}, \quad (9)$$

where R_1, R_2, A, and B all represent the material parameters of the explosive, P represents the detonation pressure, V represents the initial relative volume, and E_0 represents the initial specific internal energy. The relevant physical parameters of specific explosive materials are listed in Table 3.

4.2. Verification of Numerical Simulation Results. To verify the reliability of the numerical simulation results, taking the second field experiment as an example, the reliability of the numerical simulation results is verified by the field monitoring data.

Table 4 shows that the maximum relative error between the simulation results and the measured data is 9.05%, proving the simulation accuracy is high. However, there is an obvious difference between the numerically calculated PPV and the measured results, the reason being that the numerical method treats the surrounding rock as a homogeneous medium. Under the influence of discontinuous structural planes, the seismic waves are reflected, refracted or diffracted, resulting in a reduction in the vibration velocity. Even so, the decay trend obtained by the numerical simulation is consistent with the measured data.

Therefore, the three-dimensional numerical model established based on ANSYS/LS-DYNA can replace the field experiment to study the distribution characteristics of the blasting vibration in the tunnel.

5. Influence of Tunnel Burial Depth on Blasting Vibration Distribution Characteristics

The original design documents of the railway show that there will be some differences in the depth of the tunnel with the different excavation mileages. However, limited by factors such as the number of monitoring instruments and the accuracy of measuring instruments, it is not realistic to study the influence of burial depth on the distribution law of blasting vibration through on-site monitoring methods. In this section, numerical simulation is used to study the distribution characteristics of ground vibration caused by tunnel blasting under different tunnel burial depths to provide some theoretical suggestions for the selection of burial depths for similar tunnels.

The on-site monitoring results show that the vibration velocity at measuring point #1 is the largest. Therefore, when the tunnel burial depths are 15 m, 20 m, 25 m, 30 m, 35 m, 40 m, and 45 m, the peak vibration velocities of the particles at the corresponding positions of measuring point #1 of the numerical model are extracted. Moreover, the mathematical relationship between the peak vibration velocity of the particle and the tunnel depth is shown in Figure 9.

Table 3: Material parameters of the explosive.

Density/kg·m^{-3}	Detonation wave velocity/m·s^{-1}	A/GPa	B/GPa	R_1	R_2	E_0/GPa
1630	6930	69.3	0.254	4.15	0.950	4.98

Table 4: The comparison between the numerical calculation results and the experimental results.

Measuring point	R (m)	Field test results (cm/s)	Numerical simulation results (cm/s)	Relative error (%)
#1	27.58	1.99	1.81	9.05
#2	30.48	1.66	1.72	3.61
#3	36.89	1.34	1.44	7.46
#4	40.31	1.11	1.18	6.31
#5	49.24	1.00	1.08	8.00

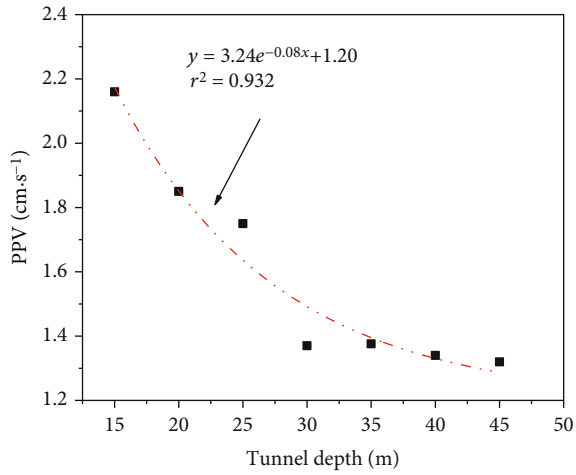

Figure 9: Relationship between tunnel depth and corresponding vibration velocity.

As shown in Figure 9, the peak vibration velocity of the particle decays exponentially with increasing tunnel burial depth, and the decay rate gradually slows with increasing distance. The expression to describe the relationship is as follows:

$$\mathrm{PPV} = 3.24\mathrm{e}^{-0.08D} + 1.20, \tag{10}$$

where PPV represents the peak velocity of the particle at measuring point #1, and D represents the tunnel burial depth. The fitting goodness of Formula (10) is 0.932, showing high fitting accuracy.

According to "Blasting Safety Regulations" GB6722-2014, the control threshold of vibration speed is 1.5 cm/s for earth caves, adobe houses, and rubble houses. According to Formula (8), the critical depth of the underpass railway tunnel is 29.74 m.

6. Conclusion

Relying on the specific railway tunnel blasting project, the characteristics of ground dynamic response induced by tunnel blasting are studied through field measurement and numerical simulation. The field measurement results show that although some vibration data exceeds the control threshold, the blasting construction will not cause resonance phenomenon. In addition, through the inverse calculation of the formula, the maximum allowable charge of blasting construction shall not exceed 21.49 kg. Numerical results confirm that tunnel burial depth has an influence on the distribution law of ground blasting vibration effects. The tunnel burial depth and the corresponding particle peak vibration velocity have an exponential function relationship. According to the "Blasting Safety Regulations" GB6722-2014, the minimum value of the buried depth of this railway tunnel is 29.74 m.

Data Availability

The data used to support the findings of this study are available from the corresponding author upon request.

Conflicts of Interest

The author declare that they have no known competing financial interests or personal relationships that could have appeared to influence the work reported in this paper.

Acknowledgments

The work described in this paper is supported by the National Natural Science Foundation of China (number: 51878242) and the Natural Science Foundation of Hebei Province (number: E2020404007).

References

[1] D. Jahed Armaghani, D. Kumar, P. Samui, M. Hasanipanah, and B. Roy, "A novel approach for forecasting of ground vibrations resulting from blasting: modified particle swarm optimization coupled extreme learning machine," *Engineering with computers*, vol. 37, no. 4, pp. 3221–3235, 2021.

[2] M. S. Abdalzaher, S. S. Moustafa, M. Abd-Elnaby, and M. Elwekeil, "Comparative performance assessments of machine-learning methods for artificial seismic sources discrimination," *IEEE Access*, vol. 9, pp. 65524–65535, 2021.

[3] S. Mishra, M. Zaid, K. S. Rao, and N. K. Gupta, "FEA of urban rock tunnels under impact loading at targeted velocity," *Geotechnical and Geological Engineering*, vol. 40, pp. 1693–1711, 2022.

[4] M. Zaid, "Dynamic stability analysis of rock tunnels subjected to impact loading with varying UCS," *Geomechanics and Engineering*, vol. 24, pp. 505–518, 2021.

[5] Q. Qin and J. Zhang, "Vibration control of blasting excavation of large cross-section highway tunnel over metro line," *Arabian Journal of Geosciences*, vol. 13, no. 17, 2020.

[6] Y. Zhao, R. L. Shan, and H. L. Wang, "Research on vibration effect of tunnel blasting based on an improved Hilbert–Huang transform," *Environment and Earth Science*, vol. 80, no. 5, pp. 1–16, 2021.

[7] X. Tian, Z. Song, and J. Wang, "Study on the propagation law of tunnel blasting vibration in stratum and blasting vibration reduction technology," *Soil Dynamics and Earthquake Engineering*, vol. 126, article 105813, 2019.

[8] H. Wang, H. Bai, Y. Zhao, D. Wang, X. Wang, and S. Wang, "The removal method of the blasting vibration signal trend item and noise," *Shock and Vibration*, vol. 2021, Article ID 1645380, 10 pages, 2021.

[9] M. S. Abdalzaher, M. S. Soliman, S. M. El-Hady, A. Benslimane, and M. Elwekeil, "A deep learning model for earthquake parameters observation in IoT system-based earthquake early warning," *IEEE Internet of Things Journal*, vol. 9, pp. 8412–8424, 2022.

[10] M. Hasanipanah, R. Naderi, J. Kashir, S. A. Noorani, and A. Zeynali Aaq Qaleh, "Prediction of blast-produced ground vibration using particle swarm optimization," *Engineering with Computers*, vol. 33, no. 2, pp. 173–179, 2017.

[11] N. Jiang, C. Zhou, S. Lu, and Z. Zhang, "Propagation and prediction of blasting vibration on slope in an open pit during underground mining," *Tunnelling and Underground Space Technology*, vol. 70, pp. 409–421, 2017.

[12] S. Kumar, A. K. Mishra, B. S. Choudhary, R. K. Sinha, D. Deepak, and H. Agrawal, "Prediction of ground vibration induced due to single hole blast using explicit dynamics," *Mining, Metallurgy & Exploration*, vol. 37, no. 2, pp. 733–741, 2020.

[13] M. I. Matidza, Z. Jianhua, H. Gang, and A. D. Mwangi, "Assessment of blast-induced ground vibration at Jinduicheng molybdenum open pit mine," *Natural Resources Research*, vol. 29, no. 2, pp. 831–841, 2020.

[14] G. Chen, Q. Li, D. Li, Z. Wu, and Y. Liu, "Main frequency band of blast vibration signal based on wavelet packet transform," *Applied Mathematical Modelling*, vol. 74, pp. 569–585, 2019.

[15] S. A. Hosseini, A. Tavana, S. M. Abdolahi, and S. Darvishmaslak, "Prediction of blast-induced ground vibrations in quarry sites: a comparison of GP, RSM and MARS," *Soil Dynamics and Earthquake Engineering*, vol. 119, pp. 118–129, 2019.

[16] D. Huang, S. Cui, and X. Li, "Wavelet packet analysis of blasting vibration signal of mountain tunnel," *Soil Dynamics and Earthquake Engineering*, vol. 117, pp. 72–80, 2019.

[17] J. Yang, J. Dai, C. Yao, S. Jiang, C. Zhou, and Q. Jiang, "Estimation of rock mass properties in excavation damage zones of rock slopes based on the Hoek-Brown criterion and acoustic testing," *International Journal of Rock Mechanics and Mining Sciences*, vol. 126, article 104192, 2020.

[18] R. Nateghi, M. Kiany, and O. Gholipouri, "Control negative effects of blasting waves on concrete of the structures by analyzing of parameters of ground vibration," *Tunnelling and Underground Space Technology*, vol. 24, no. 6, pp. 608–616, 2009.

[19] T. Ongen, D. Karakus, G. Konak, and A. H. Onur, "Assessment of blast-induced vibration using various estimation models," *Journal of African Earth Sciences*, vol. 145, pp. 267–273, 2018.